New Spacecraft-Charging Solar Array Failure Mechanism

David B. Snyder, Dale C. Ferguson, Boris V. Vayner, and Joel T. Galofaro
NASA/Lewis Research Center, Cleveland, OH 44135

Abstract Although arcing due to spacecraft charging has been known for some twenty years, and mitigation strategies have been used to prevent it, it is now known that initial arcs can lead to potentially catastrophic continuous arcs between adjacent solar cells or electrical traces. First discovered by the Loral Tempo spacecraft, this phenomenon has now also been verified in laboratory testing for the LEO EOS-AM solar arrays, which are currently being modified to prevent such occurrences on orbit. This paper will show laboratory results on mechanisms, risky configurations, and thresholds in voltages, separations, and currents as determined by vacuum plasma testing at the NASA Lewis Research Center. Mitigation strategies will also be discussed.

Introduction

Previous experience has shown that electrical discharges (arcs) occur on the surfaces of a high voltage solar array with high negative potential relative to the surrounding plasma. The most probable site for an arc inception is a triple junction: metallic interconnect, coverglass, and plasma [*Ferguson*, 1989; *Cho and Hastings*, 1991; *Jongeward and Katz*, 1998], but an arc on a triple junction can not cause a substantial damage to a solar array. However, two cases of considerable damage to solar arrays were registered during 1997 for two Space Systems/Loral high-powered spacecraft operating in GEO. Katz et al. [1998] suggested that the damage could be caused by an electrical discharge between adjacent solar cells with the highest potential difference. In this case an arc can provide enough power for local heating of a Kapton substrate up to the temperature of the polymer pyrolysis. This process can be supported by the current generated by the array itself until strings of solar cells become shorted. Comprehensive tests have been undertaken to verify the phenomenon and to elaborate the preventive actions. The same mechanism of array failure is applicable to any array with high enough both operating voltage and potential difference between adjacent solar cells. A sample of the EOS-AM solar array (operating voltage 127 V) has been tested also. Results obtained in laboratory experimentation have been used to modify the design of the array in such a way that excludes the possibility of a sustained discharge between adjacent cells.

A theoretical analysis allows us to determine the main parameters that are of critical importance for array operation. Even though some measures have been undertaken to prevent sustained arcs for the arrays mentioned above, we believe that the problem of array reliability is far from to be solved in general. For instance, we have found that arcs on triple junctions cause array performance degradation, but there are no quantitative results regarding the rate of the degradation.

2.Experimental setup

The purposes of the experiment are the following: to measure arc threshold and arc rate vs. bias voltage, to locate arc sites, to determine critical parameters such as voltage drop and maximum current between adjacent cells, and to verify the methods of the prevention of sustained arcs. The circuitry diagram is shown in Fig. 1 [*Katz*, 1997]. A digital voltmeter has been installed to measure the voltage drop between two strings during the sustained discharge (not shown in Fig.1). All measurements have been done in the large vacuum tank (1.8 m diameter and 3m length)

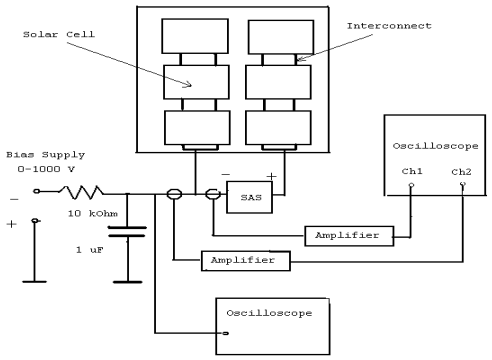

Fig.1 Solar Array Simulator (SAS) provides voltage 0 - 200 V and current 0-3 A.

with background pressure 0.1 μTorr, neutral gas (Xe) pressure 8-10 μTorr, the electron number density (3-5)10^6 cm^{-3}, and electron temperature 1-1.2 eV. The sample of solar array is installed in the middle of the chamber facing the video camera (Fig.2). All events were videotaped to allow us to locate arc sites. Six samples with different design (Si and GaAs) were tested, and all of them demonstrated similar behavior, although the magnitudes of arc thresholds, arc rates,

critical SAS currents and voltages had been rather scattered.

Fig.2. Sustained arc on GaAs array. Bias voltage –350V, SAS voltage 80 V, and current limit 2.25 A. The picture in left bottom corner is taken one second after the flash. The sustained arc remains steady until the SAS is turned off.

3.Experimental results

In this paper we present results obtained in testing one GaAs solar array sample provided by Space System/Loral. The design and cell layout for this array is shown in Fig.3.

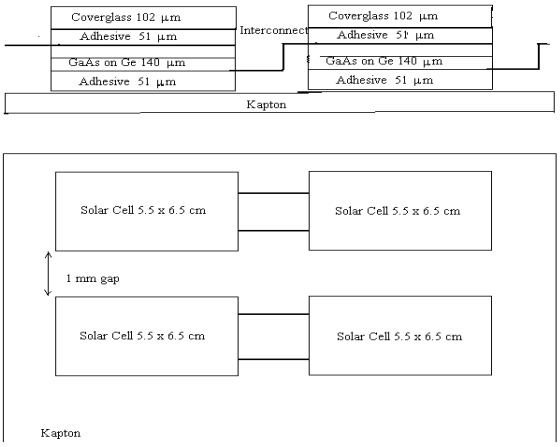

Fig.3. The GaAs Solar Array Design.

The sample consists of 36 cells arranged in 3 strings with 12 cells in each string. On the first stage of the experiment the whole sample was biased to determine the arc threshold and arc rate. Measurements have demonstrated a strong dependence of the arc rate on the bias voltage, as expected according to many previous space and ground experiments [*Ferguson*, 1989; *de la Cruz et al.*, 1996]. The arc rate grows almost a hundred times when the bias voltage changes from –170 V to –220 V (Fig. 4). It is worth noting that the curve of arc rate vs. bias voltage shifts to the right after the sample has experienced a few hundred arcs. At the end of the experiment a bias voltage about –350 V is needed to keep arc rate in the range of 02-0.3 arc/minute.

It is also in agreement with expectation that most arcs are located on triple junctions (Fig. 5). The absence of arcs in the gap between adjacent cells when the SAS is switched off is important for understanding the physical mechanisms of arc inception in the gap between cells that are biased by the SAS in the next stage of the experiment.

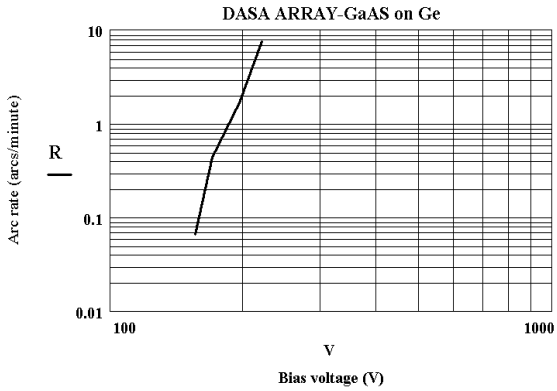

Fig.4. Arc rate vs. bias voltage (negative) for the virgin sample.

.

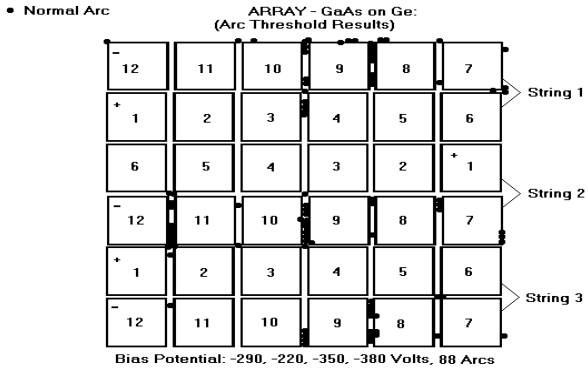

Fig.5. SAS is off. Most arc sites were on interconnects.

After a bias voltage has been applied between sections of string 2 (Fig.6) a considerable percentage of arcs occur in the gap between adjacent cells. Some of these arcs are extended , e.g. the duration of current pulse registered by the right current probe (Fig. 1) exceeds substantially the duration of the capacitor discharge current (left probe). But, because the current limit is set as low as 1.75 A, the sustained discharge between cells can not be initiated. At the end of this particular test, the current limit was set 2.25 A, and the potential difference of 80 V was high enough to keep pyrolysis steady (Fig.7).

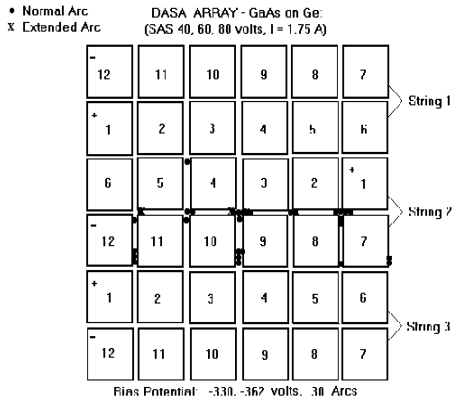

Fig.6. Arcs occur between cells due to SAS voltage

.

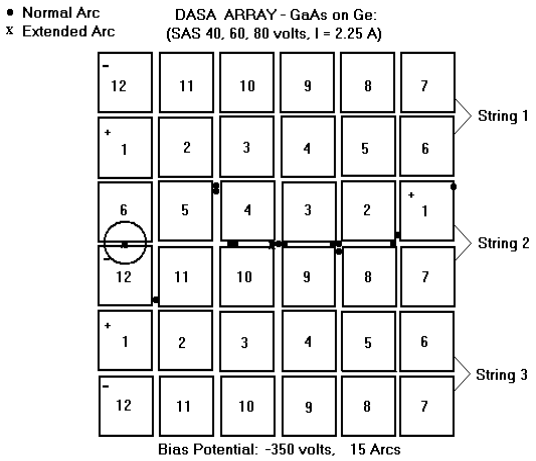

Fig.7. Sustained arc occurs between cells 6 and 12.

The results of the synchronous measurements of initial arc current, capacitor voltage, and sustained arc current are shown in Fig. 8.

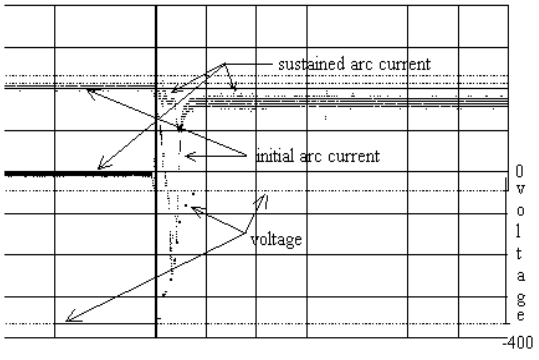

Fig. 8. The vertical scale for the initial arc current is 5 A/div, for sustained arc current- 1 A/div, and time scale is 200 μs/div.

4.Theoretical model.

The energy flux toward the Kapton substrate can be calculated from measurements of the arc current:

$$P(t) = \alpha \cdot \frac{I(t) \cdot U(t)}{2 \cdot \pi \cdot r^2} \quad \left(\frac{J}{m^2 s} \right) \qquad (1)$$

where $U(t)$ is the voltage drop on the discharge plasma cloud, r is the distance between the arc inception site and the Kapton surface, and $\alpha \leq 1$ is the numerical coefficient.

The voltage drop can be found by integrating the electrical field strength over the line connecting the arc inception site with the point on the substrate. As is well known, the initial size of the arc is about $R_0 \approx 10$ μm which is much less that the integration path (~1mm). Taking into account that the plasma conductivity $\sigma(n_e, T_e)$ depends on plasma density logarithmically (Fig.9) we obtain the following result for the voltage drop:

$$U(t) = \int_{R_0}^{\infty} \frac{I \cdot dr}{2 \cdot \pi \cdot r^2 \cdot \sigma(n_e(r), T_e)} \approx \frac{I(t)}{2\pi\sigma(T_e) R_0}$$

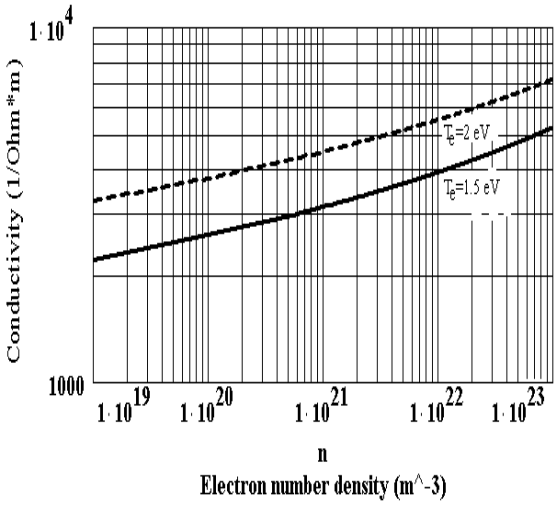

Fig.9. Plasma conductivity vs. electron number density.

The equation of thermal balance for the Kapton surface includes the heating term (Eq.(1)), and cooling terms due to radiation, thermal conductivity, and Kapton degradation. For the particular experiment (Fig. 8) the temperature of the polymer surface increases considerably in about 50 μs (Fig.10). This temperature is high enough to initiate the pyrolysis [*Ardova et al.*, 1970]. The rate of decomposition of the polymer depends on the temperature and binding energy q that allows us to calculate the neutral gas density in the gap between adjacent cells (Fig. 11). This gas contained in the space between two conductors with the potential difference 80 V provides ions and electrons to keep

the discharge steady. If we suggest the degree of ionization be about 20-50% as it usually is for a low voltage discharge, we obtain quite good agreement between the measured voltage drop and theoretical calculations (Fig.12).

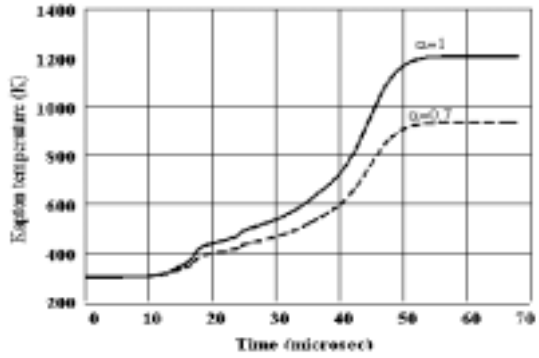

Fig.10. The increase of Kapton temperature caused by the arc.

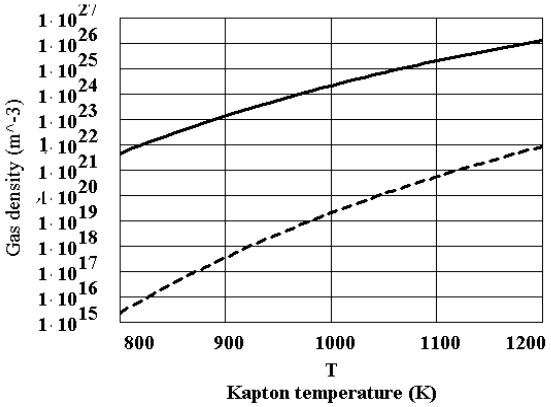

Fig. 11. Neutral gas density in the gap between adjacent cells.— q=50 kcal/mol; --- q=73 kcal/mol.

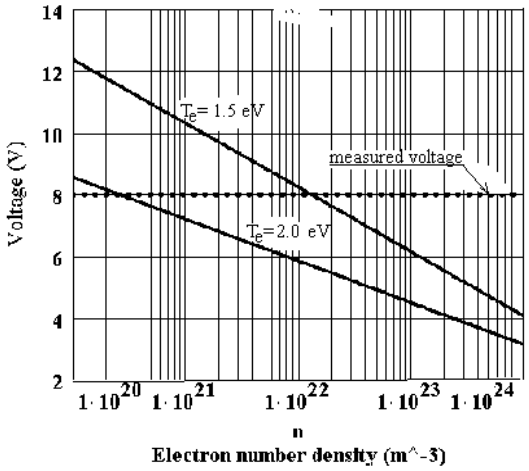

Fig.12. Theoretical calculation of the voltage drop is in good agreement with the measurement within the estimated interval of electron number density.

5. Conclusions

Comprehensive experimental tests and theoretical analysis allow us to understand physical mechanisms of solar array failure. The basic model suggested by Katz et. al. [1998] is quite adequate, and this model can be used to elaborate some measures for the prevention of a sustained discharge between adjacent cells. But before we turn our attention to preventive measures, we have to discuss the main operational parameters and their role in the arc inception (Fig. 13). The bias voltage in the experiment simulates the most negative potential of solar cells due to the spacecraft charging. This potential may reach the kilovolt range in GEO, and it is almost equal to the array operating voltage in LEO. An additional capacitor (C=1 μF, Fig. 1) simulates the capacitance of a solar array. For the particular GaAs array (Fig.3) the capacitance can be estimated as 0.1-0.2 μF/m^2. Currently, high-powered spacecraft have arrays with the area 20-30 m^2. To estimate an effective capacitance we need to take into account the distribution of the potential along an array and the fact that the entire surface of an array is not discharged during the arc. However, even a conservative estimate demonstrates that 1μF is rather the lower limit. The probability of initiation of the pyrolysis rises with an increase in the arc power ($P \propto C \cdot U_{bias}^2$) and goes down with the increase in the gap between the cells, but the arc threshold and arc rate depend on the coverglass thickness, and cell and interconnect materials; thus, changes in the array design may result in an arc threshold that is higher than the array potential with respect to the plasma. However, increases in the array size and weight are in contradiction with economical requirements. Protection of the Kapton substrate by an RTV barrier between strings results in an increase in the voltage threshold for a sustained discharge (U_{SAS}=160-200 V depending on the array design) but this solution is also not fully satisfactory. RTV coverage adds weight and cost to the array, and the question of the thermal compatibility with the array material is still unanswered. The SAS voltage simulates the potential difference between adjacent cells caused by an array operation. This value can be reduced considerably (for example, to 40 V) by a special wiring scheme. Pyrolysis can be prevented also by limiting the current that flows through the discharge area between cells. It seems that a current limit 1.5 A is low enough to achieve the expected reliability of the array. These modifications have the same disadvantages of higher cost and weight, and they do not protect an array from gradual degradation due to arcing on triple junctions. We believe that the modern tendency to raise operating voltages (above 300 V) is in obvious contradiction with the standard solar array design.

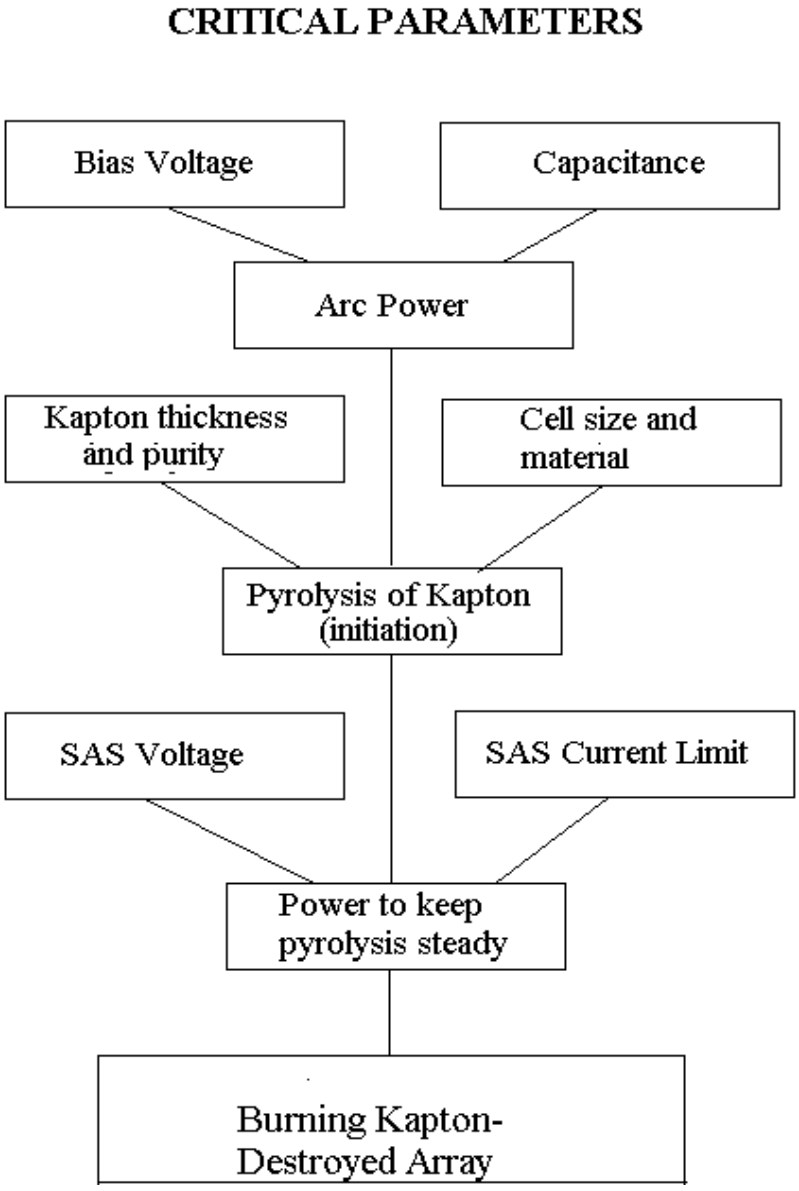

Fig. 13. Critical parameters that define the probability of an array failure.

References

Ardova, N., Bessonov, M., Laius, L.,and Rudakov, A., Polyimides: A New Class of Thermally Stable Polymers, *Progress in Material Science Series*, Vol.VII, Technomic Publ. Co., Stamford, Conn., 1970.

Cho, M., and Hastings,D.E., Dielectric Charging Processes and Arcing Rates of High-Voltage Solar Arrays, *Journal of Spacecraft and Rockets, 28,698,1991*.

de la Cruz, C.P., Hastings,D., Ferguson, D., and Hillard, B., Data Analysis and Model Comparison for Solar Array Module Interactions Experiment, *Journal of Spacecraft and Rockets, 33,438,1996*

Ferguson, D., Solar Array Arcing in Plasmas, *Third Annual Workshop on Space Operations Automation and Robotics, Houston, TX July 25-27, 1989, p.509*

Katz, I. Solar Array Arc Test. Maxwell Technical Document, August 21, 1997. Katz.,I., Davis, V., Snyder, D., and Robertson, E., ESD Triggered Solar Array Failure Mechanism *This Volume*

Jongeward, G., and Katz, I. Effect of Conduction and Ion Currents on Solar Array Arc Threshold *This Volume*